# 論文 / 著書情報
# Article / Book Information

| | |
|---|---|
| 論題(和文) | Applicable Parameter Ranges for Simplified Seismic Design of Multi-Tower Base-Isolated Structures |
| Title(English) | |
| 著者(和文) | 李晶, 佐藤大樹 |
| Authors(English) | Jing Li, Daiki Sato |
| 出典 / Citation | 日本建築学会関東支部研究報告集, I, , pp. 321-324 |
| Citation(English) | , I, , pp. 321-324 |
| 発行日 / Pub. date | 2026, 3 |
| 権利情報 | 一般社団法人 日本建築学会 |

2025年度日本建築学会
関東支部研究報告集 I
2026年3月

# Applicable Parameter Ranges for Simplified Seismic Design of Multi-Tower Base-Isolated Structures

構造一振動　　正会員 ○ 李　晶　　正会員　佐藤大樹

Multi-tower building, Base-isolated system,
Equivalent displacement spectrum, MDOF model

## 1. Introduction

To mitigate urban earthquake risks, the Japan Society of Seismic Isolation (JSSI) proposes a system wherein multiple buildings share a common isolation layer[1]. This study defines terms it Multi-Tower Base-Isolated Structure (MTBIS).

Li et al. [2] proposed the simplified equivalent ground motion derived from an SDOF model, demonstrating it generally yields safe design results. However, their validation relied on the Multiple-Building Single-Degree-of-Freedom (MS) model, which inherently simplifies each building into an SDOF system, thereby failing to account for higher-order mode effects.

In this paper, utilizing a Multiple Building Multi-Degrees-of-Freedom Model (MM model), we verify the validity of this simplified equivalent displacement spectrum. Additionally, this study quantitatively determines the applicable parameter ranges for the mass ratio and period ratio to ensure design accuracy.

## 2. Analysis Models and Input Ground Motions

### 2.1 Superstructure and Analysis Model

The analytical model comprises eleven buildings (six types) sharing a common isolation base (Figs. 1-2). Building classifications, masses, and fundamental periods are listed in Tables 1-3. Abbreviations include: low-rise building (LB), high-rise building (HB), GYM, energy center (EC), disaster command center (DC), and hospital (HOS).

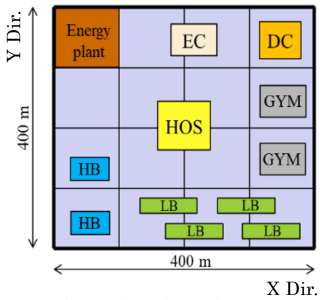

Fig. 1 Plan view of MTBIS

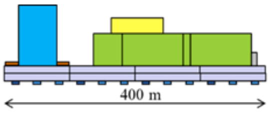

Fig. 2 Elevation view of MTBIS

Table 1 Properties of superstructures

| Building Type | Stories | Structure | Number of buildings |
|---|---|---|---|
| LB | 15 | RC | 4 |
| HB | 29 | RC | 2 |
| GYM | 5 | S | 2 |
| E | 2 | RC | 1 |
| DC | 6 | S | 1 |
| HOS | 16 | S | 1 |

Table 2 Mass of superstructures [kN·s$^2$/cm]

| LB | HB | GYM | EC | DC | HOS |
|---|---|---|---|---|---|
| 228.9 | 342.4 | 264.2 | 153.1 | 174.5 | 536.9 |

Table 3 1st period of superstructures [s]

| LB | HB | GYM | EC | DC | HOS |
|---|---|---|---|---|---|
| 0.840 | 1.526 | 0.191 | 0.419 | 0.891 | 1.676 |

This study analyzes two models: (a) the Multiple Building Multi-Degrees-of-Freedom Model (MM model), preserving superstructure MDOF characteristics; and (b) the $\Sigma m$ model, an SDOF system with total mass $\Sigma m$. For MM Model notation, stiffness and mass of the i-th floor in the $j$-th building are denoted as $k_{j,i}$ and $m_{j,i}$ respectively. Superstructure damping is stiffness-proportional ($\xi_{\mathrm{U},j}$ = 2% for Steel, 3% for RC). Isolation parameters are mass $m_0$, period $T_\mathrm{b}$, yield coefficient $\alpha_{\mathrm{h,y}}$, and viscous ratio $\xi_\mathrm{v}$.

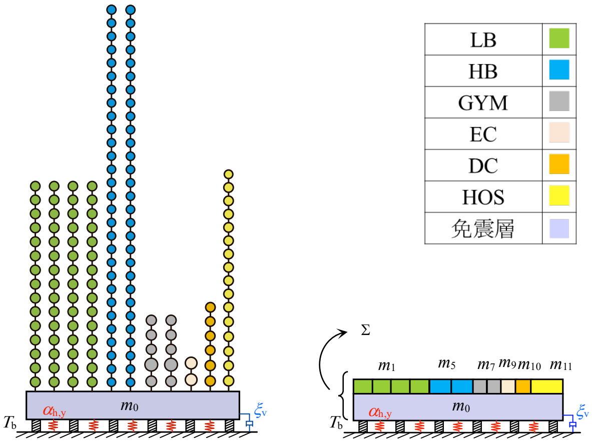

(a) MM Model　(b) $\Sigma m$ Model

Fig. 3 Analysis Model

Applicable Parameter Ranges for Simplified Seismic Design of Multi-Tower Base-Isolated Structures　　LI Jing, SATO Daiki

### 2.2 Isolation Layer

The isolation layer is designed as a rigid podium with a total area of 160,00m$^2$. Based on the structural dimensions of standard foundation beams and slabs defined in the JSSI report , the total mass of the isolation layer is estimated as $m_0$ = 16817.87 kN·s$^2$/cm. Consequently, the total system mass is $\Sigma m$ = 19811.09 kN·s$^2$/cm.

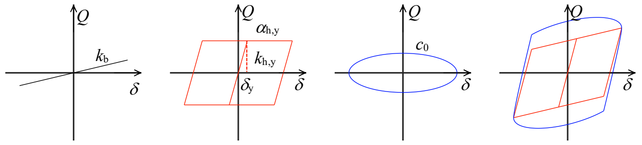

(a)isolator (b)hysteretic damper (c)viscous damper (d)isolation layer

Fig. 4 Restoring force characteristics of the isolation layer

The isolation layer incorporates linear isolators, bilinear hysteretic dampers, and linear viscous dampers. Isolator stiffness $k_b$, hysteretic damper initial elastic stiffness $k_{h,y}$, and isolation layer initial elastic stiffness $k_0$ are given by:

$$k_b = \frac{4\pi^2}{T_b^2}\Sigma m,\ k_{h,y} = \frac{\Sigma m g \alpha_{h,y}}{\delta_y},\ k_0 = k_b + k_{h,y} \tag{1-3}$$

where $T_b$ denotes isolator period, $g$ is gravitational acceleration, and $\delta_y$ is the hysteretic damper yield displacement.

Isolation layer initial elastic period $T_0$ and viscous damper damping coefficient $c_0$ are:

$$T_0 = 2\pi\sqrt{\frac{\Sigma m}{k_0}},\ c_0 = \frac{4\pi\xi_v}{T_0}\Sigma m \tag{4, 5}$$

### 2.3 Input Ground Motions

This study adopts two recorded earthquakes (El Centro 1940, Hachinohe 1968) [3], one artificial motion based on JMA KOBE 1995 EW [4] phase characteristics (Art-Kobe EW), and one synthesized wave (OS1 [5]). Spectra is presented as pseudo-velocity spectra in Fig. 5.

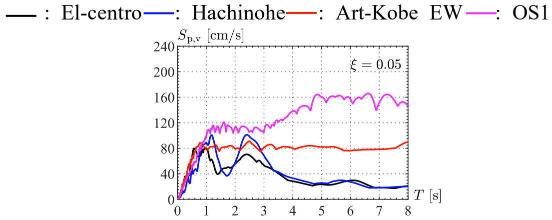

Fig. 5 Pseudo-velocity spectra

## 3. Equivalent Input Ground Motion

### 3.1 Theory of Equivalent Input Ground Motion

The dynamic equation of ground motion for the MM model is expressed as follows:

$$\mathbf{M}_{MM}\ddot{\boldsymbol{x}}_{MM} + \mathbf{C}_{MM}\dot{\boldsymbol{x}}_{MM} + \mathbf{K}_{MM}\boldsymbol{x}_{MM} = -\mathbf{M}_{MM}\ddot{x}_g\{1\}, \tag{6}$$

where $\boldsymbol{x}_{MM}$, $\dot{\boldsymbol{x}}_{MM}$, $\ddot{\boldsymbol{x}}_{MM}$, and $\ddot{x}_g$ denote displacement, velocity, acceleration, and ground acceleration respectively. Mass, damping, and stiffness matrices follow standard definitions with $N$ representing the number of superstructures.

Specifically, the mass matrix $\mathbf{M}_{MM}$ is defined by the mass matrix of the $j$-th superstructure $\mathbf{M}_j$ as follows:

$$\mathbf{M}_{MM} = \mathrm{diag}\left(m_0, \mathbf{M}_1, \ldots, \mathbf{M}_j, \ldots, \mathbf{M}_N\right) \tag{7}$$

$$\mathbf{M}_j = \mathrm{diag}\left(m_{j,1}, \ldots, m_{j,i}, \ldots, m_{j,N}\right). \tag{8}$$

The stiffness matrix $\mathbf{K}_{MM}$ is defined by the vector $\mathbf{k}_{\mathrm{base},j}$ and the stiffness matrix of the $j$-th superstructure $\mathbf{K}_j$ as follows:

$$\mathbf{K}_{MM} = \begin{bmatrix} k_0 + \sum_{j=1}^{N} k_{j,1} & \mathbf{k}_{\mathrm{base},1} & \cdots & \mathbf{k}_{\mathrm{base},N} \\ \mathbf{k}_{\mathrm{base},1}^T & \mathbf{K}_1 & & \mathbf{0} \\ \vdots & & \ddots & \\ \mathbf{k}_{\mathrm{base},N}^T & \mathbf{0} & & \mathbf{K}_N \end{bmatrix} \tag{9}$$

$$\mathbf{k}_{\mathrm{base},j} = \begin{bmatrix} -k_{j,1} & 0 & \ldots & 0 \end{bmatrix}, \tag{10}$$

$$\mathbf{K}_j = \begin{bmatrix} k_{j,1} + k_{j,2} & -k_{j,2} & 0 & \ldots & 0 \\ -k_{j,2} & k_{j,2} + k_{j,3} & -k_{j,3} & \ldots & 0 \\ 0 & -k_{j,3} & k_{j,3} + k_{j,4} & \ldots & 0 \\ \vdots & \vdots & \vdots & \ddots & -k_{j,n} \\ 0 & 0 & 0 & -k_{j,n} & k_{j,n}. \end{bmatrix} \tag{11}$$

The damping matrix $\mathbf{C}_{MM}$ is defined by the vector $\mathbf{c}_{\mathrm{base},j}$ and the stiffness matrix of the $j$-th superstructure $\mathbf{C}_j$ as follows:

$$\mathbf{C}_{MM} = \begin{bmatrix} c_0 + \sum_{j=1}^{N} c_{j,1} & \mathbf{c}_{\mathrm{base},1} & \cdots & \mathbf{c}_{\mathrm{base},N} \\ \mathbf{c}_{\mathrm{base},1}^T & \mathbf{C}_1 & & \mathbf{0} \\ \vdots & & \ddots & \\ \mathbf{c}_{\mathrm{base},N}^T & \mathbf{0} & & \mathbf{C}_N \end{bmatrix} \tag{12}$$

$$\mathbf{c}_{\mathrm{base},j} = \begin{bmatrix} -c_{j,1} & 0 & \ldots & 0 \end{bmatrix}, \tag{13}$$

$$\mathbf{C}_j = \begin{bmatrix} c_{j,1} + c_{j,2} & -c_{j,2} & 0 & \ldots & 0 \\ -c_{j,2} & c_{j,2} + c_{j,3} & -c_{j,3} & \ldots & 0 \\ 0 & -c_{j,3} & c_{j,3} + c_{j,4} & \ldots & 0 \\ \vdots & \vdots & \vdots & \ddots & -c_{j,n} \\ 0 & 0 & 0 & -c_{j,n} & c_{j,n} \end{bmatrix} \tag{14}$$

where, $c_{j,i}$ is the damping of $i$-th story for $j$-th superstructure and as follow:

$$c_{j,i} = 2\xi_{j,i}\sqrt{m_{j,i}k_{j,i}}. \tag{15}$$

Substituting these matrices into Eq. (6) yields the rearranged equation of motion for the $j$-th superstructure:

$$\mathbf{M}_j\ddot{\boldsymbol{\delta}}_j + \mathbf{C}_j\dot{\boldsymbol{\delta}}_j + \mathbf{K}_j\boldsymbol{\delta}_j = -\mathbf{M}_j\left(\ddot{x}_g + \ddot{\boldsymbol{x}}_{MM,0}\right), \tag{16}$$

where, $\ddot{\boldsymbol{x}}_{MM,0}$ is the acceleration of isolation layer for MM model. $\boldsymbol{\delta}_j$, $\dot{\boldsymbol{x}}_{MM}$, $\ddot{\boldsymbol{x}}_{MM}$ are displacement, velocity, and acceleration of the $j$-th story relative to the isolation layer.

$$\boldsymbol{\delta}_j = \boldsymbol{x}_{MM} - \boldsymbol{x}_{MM,0}, \tag{17}$$

$$\dot{\boldsymbol{\delta}}_j = \dot{\boldsymbol{x}}_{MM} - \dot{\boldsymbol{x}}_{MM,0}, \tag{18}$$

$$\ddot{\boldsymbol{\delta}}_j = \ddot{\boldsymbol{x}}_{MM} - \ddot{\boldsymbol{x}}_{MM,0}. \tag{19}$$

Regarding the response of the isolation layer, the equation can be rearranged as:

$$\Sigma m\ddot{x}_{\mathrm{MM},0} + c_0\dot{x}_{\mathrm{MM},0} + k_0 x_{\mathrm{MM},0} = -\Sigma m\left(\ddot{x}_{\mathrm{g}} + \frac{1}{\sum m}\sum_{j=1}^{N}\sum_{i=1}^{N_{\mathrm{S},j}} m_i \ddot{\delta}_{j,i}\right). \tag{20}$$

Therefore, isolation layer absolute acceleration may serve as seismic excitation for superstructure design. This acceleration is termed equivalent ground motion. The equivalent input ground motion is

$$\ddot{x}_{\mathrm{g,\,eq}} = \ddot{x}_{\mathrm{g}} + \ddot{x}_{\mathrm{MM},0} \tag{22}$$

Moreover, the equation of motion for the isolation layer can be decoupled and simplified into a SDOF model, the $\Sigma m$ Model (Fig.3.b), governed by:

$$\Sigma m\ddot{x}_{\mathrm{SDOF}} + c_0\dot{x}_{\mathrm{SDOF}} + k_0 x_{\mathrm{SDOF}} = -\Sigma m\ddot{x}_{\mathrm{g}}. \tag{21}$$

Similarly, the simplified equivalent ground motion is

$$\ddot{x}_{\mathrm{g,\,seq}} = \ddot{x}_{\mathrm{g}} + \ddot{x}_{\mathrm{SDOF}}. \tag{23}$$

When the influence of the superstructure on the isolation layer is minor, the following equation holds:

$$\ddot{x}_{\mathrm{g,\,seq}} \approx \ddot{x}_{\mathrm{g,\,eq}} \tag{24}$$

### 3.2 Equivalent Displacement spectra and Verification

By converting the equivalent ground motions (Eq. 24) into spectra ($S_{\mathrm{D,eq}}$ and $S_{\mathrm{D,seq}}$) and comparing them with the MM model's equivalent inter-story drift $\delta_{\mathrm{Ueq},\,j}$ (Fig. 6), the applicable isolation parameter range for the simplified design method is determined.

The equivalent height $H_{\mathrm{eq},\,j}$ for the $j$-th building is shown in Fig. 6 and calculated by Eq. (25). Here, $H_{j,i}$ and $\phi_{1,j,i}$ represent, height, and first-mode shape of the $i$-th story, respectively.

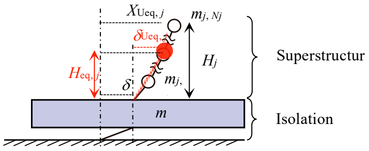

Fig. 6 Diagram of equivalent height and equivalent inter-story drift

$$H_{\mathrm{eq},\,j} = \frac{\sum_{i=1}^{N_j} m_{j,i}\phi_{1,j,i}H_{j,i}}{\sum_{i=1}^{N_j} m_{j,i}\phi_{1,j,i}} \tag{25}$$

The period of isolation layer $T_0$ and the mass ratio $\gamma_{\mathrm{m}}$ are adopted as evaluation indexs. The mass ratio $\gamma_{\mathrm{m}}$ is

$$\gamma_{\mathrm{m}} = \left|m_j\right|_{\max} / \Sigma m = m_{\mathrm{HOS}} / \Sigma m. \tag{26}$$

Figs. 7-11 show the comparison between the equivalent displacement spectrum ($S_{\mathrm{D,eq}}$) and the proposed simplified equivalent displacement spectrum ($S_{\mathrm{D,seq}}$) under varying isolation periods ($T_0$) and mass ratios ($\gamma_{\mathrm{m}}$) for different input ground motions. The solid lines represent the spectra, while the markers denote the maximum displacement responses of various superstructures. The symbols indicate the prediction accuracy ratio ($r_j = \delta_{\mathrm{Ueq},j} / S_{\mathrm{D,seq}}(T_{\mathrm{U,j}})$), where circles represent high accuracy ($0.9 \le r \le 1.1$). As consistently observed across these figures (indicated by the green dashed frames), within the range of $T_0 \ge 4$ s and $\gamma_{\mathrm{m}} \le 3\%$, the simplified spectrum ($S_{\mathrm{D,seq}}$) shows excellent agreement with the rigorous spectrum

## 4. Conclusion

This study verified the simplified equivalent displacement spectrum for MTBIS using the MM model. By analyzing the intersection of results across multiple seismic records, the simplified equivalent displacement spectrum maintains high accuracy (error within 10%) when $T_0 \ge 4$ s and $\gamma_{\mathrm{m}} \le 3\%$.

**References**

1) 日本免震構造協会 ： 免震によるレジリエントな都市の実現を目指して～レジリエントな都市の実現構想研究会免震システム技術WG 活動報告書～ , 2023.5
2) 李晶，他 2 名：複数建物を有する街区免震の設計手法:その 1 上部構造の等価入力地震波の提案，日本建築学会関東支部研究報告集, 2024.3
3) 一般社団法人建築性能基準推進協会 ： 代表的な観測地震波（加速度データ）の頒布について
4) 国土交通省 ： 強震波形（平成 7 年(1995 年)兵庫県南部地震）https://www.data.jma.go.jp/eqev/data/kyoshin/jishin/hyogo_nanbu/index.html
5) 国土交通省 ： 「長周期地震動への対策」における『基整促波』の作成, 2017.4

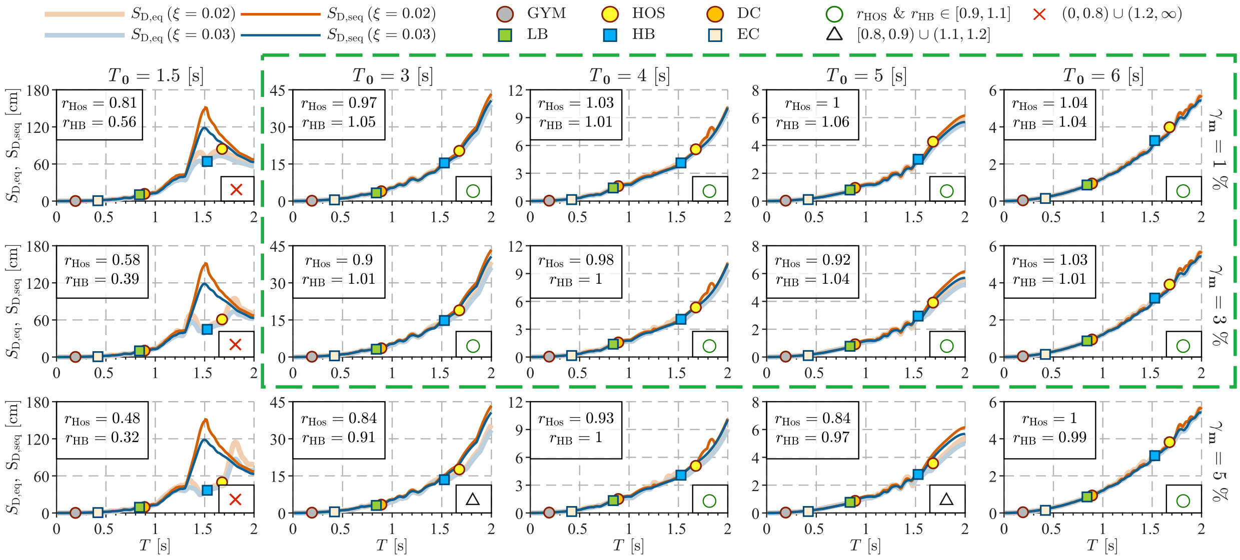

Fig. 7 Comparison between $S_{\mathrm{D,eq}}$ and $S_{\mathrm{D,seq}}$ (El Centro, $\xi_{\mathrm{v}}$ = 2%)

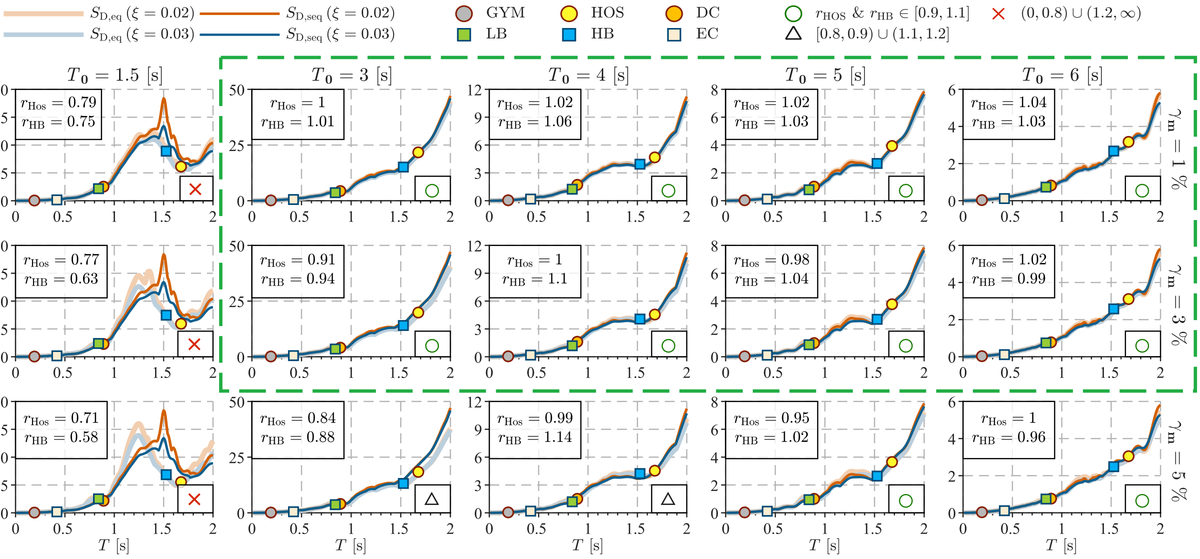

Fig. 8 Comparison between $S_{\mathrm{D,eq}}$ and $S_{\mathrm{D,seq}}$ (Hchinohe, $\xi_{\mathrm{v}} = 2\%$)

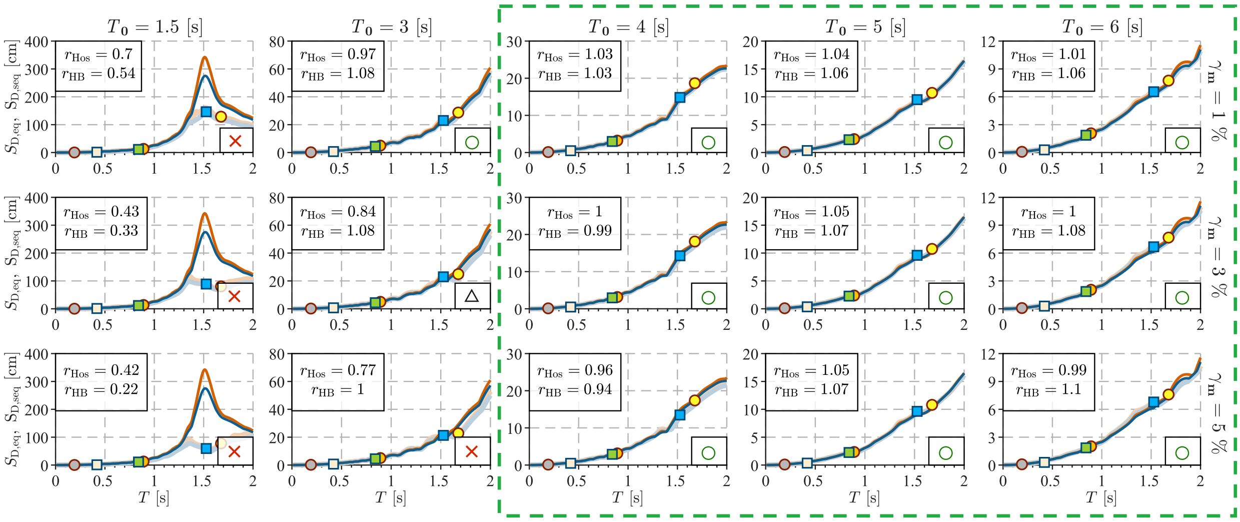

Fig. 9 Comparison between $S_{\mathrm{D,eq}}$ and $S_{\mathrm{D,seq}}$ (Art-Kobe EW, $\xi_{\mathrm{v}} = 2\%$)

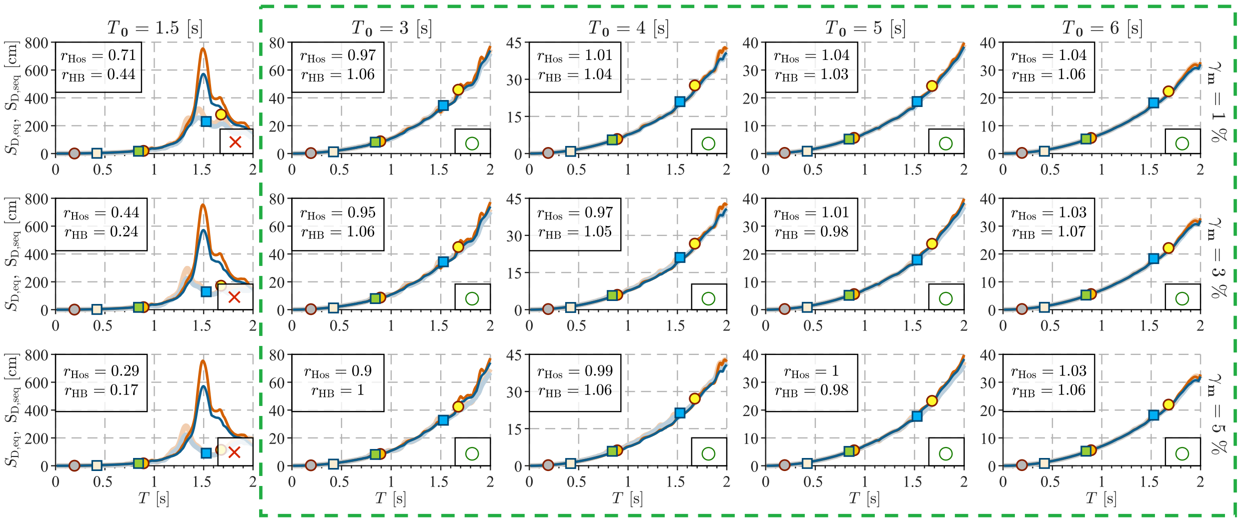

Fig. 10 Comparison between $S_{\mathrm{D,eq}}$ and $S_{\mathrm{D,seq}}$ (OS1, $\xi_{\mathrm{v}} = 2\%$)

---

＊1　東京科学大学　大学環境· 社会理工学院　大学院生

＊2　東京科学大学　准教授· 博士（工学）

*Graduate Student, Institute of Science Tokyo

*Associate Prof. , FIRST, Institute of Science Tokyo, Dr. Eng.